We are IntechOpen, the world's leading publisher of Open Access books Built by scientists, for scientists

4,800
Open access books available

122,000
International authors and editors

135M
Downloads

Our authors are among the

154
Countries delivered to

TOP 1%
most cited scientists

12.2%
Contributors from top 500 universities

CLARIVATE ANALYTICS BOOK CITATION INDEX INDEXED

WEB OF SCIENCE™

Selection of our books indexed in the Book Citation Index in Web of Science™ Core Collection (BKCI)

Interested in publishing with us?
Contact book.department@intechopen.com

Numbers displayed above are based on latest data collected.
For more information visit www.intechopen.com

7

Measurement Analysis and Diagnosis for Robot Manipulators using Advanced Nonlinear Control Techniques

Amr Pertew, Ph.D, P.Eng.
Computer and Systems Engineering Department, University of Alexandria
Egypt

Horacio Marquez, Ph. D, P. Eng and Qing Zhao, Ph. D, P. Eng
Electrical and Computer Engineering Department, University of Alberta
Canada

1. Introduction

The *measurement analysis and diagnosis problem* is gaining increasing consideration worldwide in both theory and application. This is due to the growing demand for higher reliability in control systems, and hence the importance of having a monitoring system that detects any existing measurement errors, and indicates their location and significance in the control loop. The observer-based approach is one of the most popular techniques used for fault diagnosis in general and for the measurement error diagnosis problem in particular. Many standard observer-based techniques exist in the literature providing different solutions to both the theoretical and practical aspects of the problem for the *Linear Time-Invariant* (LTI) case (see (Frank, 1990; Willsky, 1976) for good surveys on this subject). The main idea behind the observer-based approach is to estimate the outputs of the system from the measurements by using either *static gain* observers in a deterministic framework (Zhong et al., 2003) or *Kalman* filters in a stochastic framework (Chen et al., 2003). The output estimation error is then used as the residual signal, which can be analyzed further to obtain an accurate estimation of the measurement errors which affect the control system. Unlike the LTI case, however, the nonlinear problem lacks a universal approach and is currently an active area of research (see (Adjallah et al., 1994; Garcia & Frank, 1997; Hammouri et al., 1999; Kabore & Wang, 2001; Vemuri, 2001; Wang et al., 1997; Yu & Shields, 1996) for important results in this direction). The main obstacle in the solution of the observer-based nonlinear fault detection problem is the lack of a universal approach for nonlinear observer synthesis. Robot manipulators, characterized by largely nonlinear dynamics, are no exception to this dilemma and therefore need a unified framework for measurement error detection and diagnosis.
The well known Euler-Lagrange model of a robot manipulator is as follows (Sciavicco & Sicliano, 1989):

$$u = M(\theta)\,\ddot{\theta} + V(\theta, \dot{\theta}) \tag{1}$$

where θ, $\dot{\theta}$ and $\ddot{\theta} \in \mathbb{R}^n$ are vectors representing the position, velocity and acceleration of the n-link robot respectively, and $u \in \mathbb{R}^n$ represents the actuator torques. By defining the state variables as $x_1 = \theta$, $x_2 = \dot{\theta}$, we get the state space model:

$$\dot{x} = f(x) + g(x)u \tag{2}$$

where $x = \begin{bmatrix} x_1 \\ x_2 \end{bmatrix}$, $f(x) = \begin{bmatrix} x_2 \\ -M^{-1}(x_1)V(x_1, x_2) \end{bmatrix}$ and $g(x) = \begin{bmatrix} 0_n \\ M^{-1}(x_1) \end{bmatrix}$. This model clearly shows the nonlinearities resulting from the inertia matrix $M(\theta)$, and from the vector $V(\theta, \dot{\theta})$ which combines all the centrifugal, coriolis, gravity and friction terms that are an integral part of the manipulator dynamical equations.
The problem of measurement error diagnosis for robot manipulators described by the Euler-Lagrange model is an interesting one. Sensor faults could affect both the position and velocity measurements, and would have a detrimental effect on the control performance. The dynamic observer structure which was introduced in (Pertew et al., 2006; 2007) can serve as a general framework for solving this problem. Necessary and sufficient design conditions for the problem of error detection can be derived from the nonlinear dissipativity properties inherent in the robot structure. Another important advantage of this approach stems from combining the objectives of estimating the error magnitudes, as well as detecting and isolating the error sources. Using the extra degrees of freedom in the dynamic observer structure, the problem is solvable by minimizing the fault effects in a narrow frequency band on the observer's estimation error. This is an important advantage of the new framework over the classical constant gain structure. The robot manipulator measurement error diagnosis problem could then be generally modelled as a convex optimization problem and solved using a standard *Linear Matrix Inequality* (LMI) design procedure. Using standard weightings, different frequency patterns for the measurement errors can also be considered.

2. Nonlinear Observers and Terminology

An important class of nonlinear systems is:

$$\dot{x}(t) = Ax(t) + \Gamma(u, t) + \Phi(x, u, t) \tag{3}$$

$$y(t) = Cx(t) + f(t),\ A \in \mathbb{R}^{n \times n},\ C \in \mathbb{R}^{p \times n} \tag{4}$$

where (A, C) detectable, $f(t)$ represent measurement errors, and $\Phi(x, u, t)$ satisfies:

$$\| \Phi(x_1, u, t) - \Phi(x_2, u, t) \| \leq \alpha \| x_1 - x_2 \| \tag{5}$$

$\forall u \in \mathbb{R}^m$ and $t \in \mathbb{R}$ and $\forall x_1$ and $x_2 \in D$, where D is a closed and bounded region containing the origin. These systems have been widely referred to as nonlinear Lipschitz systems, due to the Lipschitz continuity condition in (5) that affect them. Due to their importance and the variety of nonlinear systems that they cover, much effort has been done towards solving the observer design problem for this class of nonlinear systems. One important advantage is that robot manipulators fall in the class of nonlinear Lipschitz systems. The classical observer structure for Lipschitz systems of the form (3)-(5), with no measurement errors is the well-known Luenberger structure, represented by the following equations:

$$\dot{\hat{x}} = A\hat{x} + \Gamma(u, t) + \Phi(\hat{x}, u, t) + L(y - \hat{y}),\ L \in \mathbb{R}^{n \times p} \tag{6}$$

$$\hat{y} = C\hat{x} \tag{7}$$

A more general framework introduced in (Pertew et al., 2006), makes use of dynamical observers of the form:

$$\dot{\hat{x}} = A\hat{x} + \Gamma(u,t) + \Phi(\hat{x},u,t) + \eta \tag{8}$$

$$\dot{\xi} = A_L\xi + B_L(y-\hat{y}),\ A_L \in \mathbb{R}^{k\times k},\ B_L \in \mathbb{R}^{k\times p} \tag{9}$$

$$\eta = C_L\xi + D_L(y-\hat{y}),\ C_L \in \mathbb{R}^{n\times k},\ D_L \in \mathbb{R}^{n\times p} \tag{10}$$

$$\hat{y} = C\hat{x} \tag{11}$$

We will write $K = \left[\begin{array}{c|c} A_L & B_L \\ \hline C_L & D_L \end{array}\right]$ to represent the dynamic observer gain in (23)-(24). It can be shown that K, sufficient to achieve observer convergence, can be represented by a set of controllers. This design freedom can be used in the measurement error diagnosis problem discussed in this chapter, by analyzing the residual signal:

$$r(t) = y(t) - \hat{y}(t) \tag{12}$$

This will be discussed in details throughout this chapter. To this end, the following definitions and notation are widely accepted and used by the *Fault Detection and Diagnosis* (FDD) community:

Definition 1. *Fault detection: The residual in equation (12) achieves fault detection (strong fault detection) if the following condition is satisfied:*
$r(t) = 0\ ;\ \forall t$ *if (if and only if)* $f(t) = 0\ ;\ \forall t$

Definition 2. *Fault isolation: The residual in (12) achieves fault isolation if:*
$(r_i(t) = 0\ ;\ \forall t \iff f_i(t) = 0\ ;\ \forall t)$ *; for* $i = 1, \cdots, p$

Definition 3. *Fault identification: Fault identification is satisfied by (12) if:*
$(r_i(t) = f_i(t)\ ;\ \forall t)$ *; for* $i = 1, \cdots, p$

The previous definitions are borrowed from (Chen & Patton, 1999). Note that, in these definitions, the transient period of the residual signal is not considered, and that since the focus in this chapter is on sensor faults the term "measurement error" will be used instead of "fault" throughout the chapter.
The following definition and notation will also be used in this chapter:

Definition 4. *$\mathcal{L}_2$ space: Space $\mathcal{L}_2$ consists of all Lebesgue measurable functions $u : \mathbb{R}^+ \to \mathbb{R}^q$, with finite $\|u\|_{\mathcal{L}_2}$, where* $\|u\|_{\mathcal{L}_2} \triangleq \sqrt{\int_0^\infty \| u(t) \|^2 \ \mathrm{d}t}$.

For a system $H : \mathcal{L}_2 \to \mathcal{L}_2$, we will represent by $\gamma(H)$ the $\mathcal{L}_2$ gain of H defined by $\gamma(H) = \sup_u \frac{\|Hu\|_{\mathcal{L}_2}}{\|u\|_{\mathcal{L}_2}}$. It is well known that, for a LTI system $H : \mathcal{L}_2 \to \mathcal{L}_2$ (with a transfer matrix $\hat{H}(s)$), $\gamma(H) \equiv \| \hat{H}(s) \|_\infty \triangleq \sup_{\omega\in\mathbb{R}} \sigma\max(\hat{H}(j\omega))$. The matrices I_n, 0_n and 0_{nm} will represent the identity matrix of order n, the zero square matrix of order n and the zero n by m matrix respectively. $Diag_r$(a) represents the diagonal square matrix of order r with $\begin{bmatrix} a & a & \cdots & a \end{bmatrix}_{1\times r}$ as its diagonal vector, while $diag(a_1,\ a_2, \cdots,\ a_r)$ represents the one with $\begin{bmatrix} a_1 & a_2 & \cdots & a_r \end{bmatrix}$ as its diagonal vector. $\hat{T}_{yu}$ represents the transfer matrix

from input u to output y. RH_∞ denotes the space of all proper real rational stable transfer matrices. The partitioned matrix $H = \left[\begin{array}{c|c} A & B \\ \hline C & D \end{array}\right]$ (when used in $y = Hu$) represents ($\dot{\xi} = A\xi + Bu,\ y = C\xi + Du$), and $\hat{H}(s)$=$C(sI - A)^{-1}B + D$. We will make use of (13) (Zhou & Doyle, 1998), if s is not an eigenvalue of A:

$$\text{rank}\begin{bmatrix} A - sI & B \\ C & D \end{bmatrix} = n + \text{rank}\left(\hat{H}(s)\right),\ n \text{ being the dimension of } A \tag{13}$$

The setup in Fig. 1 will also be used throughout the chapter along with:

$$G = \left[\begin{array}{c|cc} A & B_1 & B_2 \\ \hline C_1 & D_{11} & D_{12} \\ C_2 & D_{21} & D_{22} \end{array}\right] \tag{14}$$

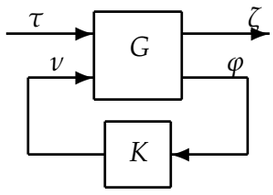

Fig. 1. Standard setup.

We will also make use of the following result from (Gahinet & Apkarian, 1994):

Theorem 1. *Assume stabilizability and detectability of* (A, B_2, C_2) *and that* $D_{22} = 0$, *and let* $\mathcal{N}_{12}$ *and* $\mathcal{N}_{21}$ *denote orthonormal bases of the null spaces of* $\left(B_2^T, D_{12}^T\right)$ *and* (C_2, D_{21}). *There exists a controller* K *such that* $\|\hat{T}_{\zeta\tau}\|_\infty < \gamma$ *if and only if there exist symmetric* $R, S \in \mathbb{R}^{n\times n}$ *satisfying the system of LMIs:*

$$\left[\begin{array}{c|c} \mathcal{N}_{12} & 0 \\ \hline 0 & I \end{array}\right]^T \left[\begin{array}{cc|c} AR + RA^T & RC_1^T & B_1 \\ C_1R & -\gamma I & D_{11} \\ \hline B_1^T & D_{11}^T & -\gamma I \end{array}\right] \left[\begin{array}{c|c} \mathcal{N}_{12} & 0 \\ \hline 0 & I \end{array}\right] < 0 \tag{15}$$

$$\left[\begin{array}{c|c} \mathcal{N}_{21} & 0 \\ \hline 0 & I \end{array}\right]^T \left[\begin{array}{cc|c} A^TS + SA & SB_1 & C_1^T \\ B_1^TS & -\gamma I & D_{11}^T \\ \hline C_1 & D_{11} & -\gamma I \end{array}\right] \left[\begin{array}{c|c} \mathcal{N}_{21} & 0 \\ \hline 0 & I \end{array}\right] < 0 \tag{16}$$

$$\begin{bmatrix} R & I \\ I & S \end{bmatrix} \geq 0 \tag{17}$$

3. Robot Manipulator Measurement Error Detection

As mentioned earlier, robot manipulators fall in the category of nonlinear Lipschitz systems. This is clear by rewriting the robot manipulator model in (2) as:

$$\dot{x} = Ax + \Phi(x, u, t) \tag{18}$$

where $A = \begin{bmatrix} 0_n & I_n \\ 0_n & 0_n \end{bmatrix}$, $\Phi = \begin{bmatrix} 0_n \\ M^{-1}(x_1)u - M^{-1}(x_1)V(x_1, x_2) \end{bmatrix}$. It is important to note that the nonlinear terms in Φ are mainly trigonometric terms which are locally Lipschitz, and an upper bound on the Lipschitz constant can be found by computing $\|\partial\Phi(x,u,t)/\partial x\|$ over the operating range (Marquez, 2003). Another representation of (2) around an operating point x^* of interest is:

$$\dot{x} = Ax + Bu + \Phi(x,u,t) \tag{19}$$

where $A = \left(\frac{\partial f}{\partial x}\right)|_{x^*}$, $B = \left(\frac{\partial g}{\partial x}\right)|_{x^*}$, $\Phi = (f(x) - Ax + g(x)u - Bu)$.
It is also important to note that (18) and (19) are both exact models of (2). By neglecting the terms in Φ in (19), one gets the well known approximate linearized model around the operating point x^*, i.e:

$$\dot{x} = Ax + Bu \tag{20}$$

where $A = \left(\frac{\partial f}{\partial x}\right)|_{x^*}$, $B = \left(\frac{\partial g}{\partial x}\right)|_{x^*}$, which is an approximate model of (2). In the formulation used in this chapter, however, no approximation is needed and the exact Lipschitz model in (19) can be directly use for solving the measurement error diagnosis problem.
Starting by the measurement error detection problem represented by Definition 1, the robot measurements are assumed to be any linear combination of the position and velocity sensors which satisfies the detectability condition needed for observer design. Errors in measurements affect the system, and the purpose is to design an observer which satisfies the measurement error detectability condition as per Definition 1. By making use of dynamical observers of the form:

$$\dot{\hat{x}}(t) = A\hat{x}(t) + \Gamma(u,t) + \Phi(\hat{x},u,t) + \eta(t) \tag{21}$$
$$\hat{y}(t) = C\hat{x}(t) \tag{22}$$

where $\eta(t)$ is obtained by applying a dynamical compensator K of order k ("k" being arbitrary) on the output estimation error. In other words $\eta(t)$ is given from

$$\dot{\xi} = A_L\xi + B_L(y - \hat{y}),\ A_L \in \mathbb{R}^{k\times k},\ B_L \in \mathbb{R}^{k\times p} \tag{23}$$
$$\eta = C_L\xi + D_L(y - \hat{y}),\ C_L \in \mathbb{R}^{n\times k},\ D_L \in \mathbb{R}^{n\times p} \tag{24}$$

We will also write

$$K = \left[\begin{array}{c|c} A_L & B_L \\ \hline C_L & D_L \end{array}\right] \tag{25}$$

to represent the compensator in (23)-(24). It is straightforward to see that this observer structure reduces to the usual observer in (6)-(7) when $K = \left[\begin{array}{c|c} 0_k & 0_{kp} \\ \hline 0_{nk} & L \end{array}\right]$. The additional dynamics brings additional degrees of freedom in the design, something that could be used to add the measurement error detection objective to the state estimation problem in the observer design. The observer error dynamics is now given by

$$\dot{e}(t) = A\,e + \Phi(x,u,t) - \Phi(\hat{x},u,t) - \eta(t) \tag{26}$$
$$r(t) = Ce(t) + f(t) \tag{27}$$

which can also be represented by the setup in Fig. 1 where G has the state space representation in (14) with appropriate matrices and with the following variables:

$$\tau = \tilde{\phi} = \Phi(x,u,t) - \Phi(\hat{x},u,t),\ \zeta = e = x - \hat{x},\ \nu = \eta = K(y - \hat{y}),\ \text{and}\ \varphi = y - \hat{y} \quad (28)$$

We denote by $\hat{T}_{\zeta\tau}$ the transfer function between τ and ζ for this setup. The following theorem provides a general solution to the dynamic observer condition needed to achieve measurement error detection:

Theorem 2. *Given the nonlinear system in (3)-(5), the residual signal in (8)-(12) achieves measurement error detection, $\forall\ \Phi$ satisfying the Lipschitz condition in (5) with a Lipschitz constant α, if the observer gain K is chosen such that: $sup_{\omega\in\mathbb{R}}\ \sigma_{max}[\hat{T}_{\zeta\tau}(j\omega)] < \frac{1}{\alpha}$.*

Proof: The proof is built on proving that, when the measurement error vector $f = 0$, the state $\hat{x}$ of the observer (8)-(11) asymptotically converges to the system state x for all $\Phi(x,u,t)$ satisfying (5) with a Lipschitz constant α if the dynamic observer gain K is chosen s.t:

$$sup_{\omega\in\mathbb{R}}\ \sigma_{max}[\hat{T}_{\zeta\tau}(j\omega)] < \frac{1}{\alpha} \quad (29)$$

Using the variable definitions in (28) it can be seen that $\hat{T}_{\zeta\tau}$ can be represented as:

$$\hat{T}_{\zeta\tau} = \hat{T}_{e\tilde{\phi}} = \left[\begin{array}{cc|c} A - D_L C & -C_L & I_n \\ B_L C & A_L & 0_{kn} \\ \hline I_n & 0_{nk} & 0_n \end{array}\right] \quad (30)$$

and is such that $\gamma(\hat{T}_{e\tilde{\phi}}) = \| \hat{T}_{e\tilde{\phi}} \|_\infty < \frac{1}{\alpha}$ according to (29). The proof for sufficiency follows from noting that the estimation error e is given from the feedback interconnection of $\hat{T}_{e\tilde{\phi}}$ and Δ as shown in Fig. 2 where Δ is the static nonlinear time-varying operator defined as follows:

$$\begin{aligned} \Delta(t) : e \rightarrow \tilde{\phi} &= \Phi(x,u,t) - \Phi(\hat{x},u,t) \\ &= \Phi(e + \hat{x}(t), u(t), t) - \Phi(\hat{x}(t), u(t), t) \end{aligned}$$

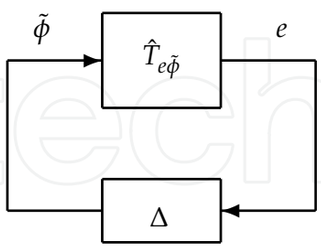

Fig. 2. Feedback interconnection.

In this loop, $\gamma(\hat{T}_{e\tilde{\phi}}) < \frac{1}{\alpha}$ as mentioned earlier. Although an exact expression for Δ is not available, we have $\gamma(\Delta) \leq \alpha$ as from the Lipschitz condition in (5) it follows that

$$\gamma(\Delta) \leq \frac{\sqrt{\int_0^\infty \alpha^2 \parallel x - \hat{x} \parallel^2 \ \mathrm{d}t}}{\sqrt{\int_0^\infty \parallel x - \hat{x} \parallel^2 \ \mathrm{d}t}} \quad \leq \alpha$$

Using the bounds on the $\mathcal{L}_2$ gains of the operators $\hat{T}_{e\tilde{\phi}}$ and Δ, nonlinear dissipativity of the feedback interconnection is satisfied, by noting the following properties for the feedback loop in Fig. 2:

(a) Δ is a static nonlinearity (no internal states) and $\hat{T}_{e\tilde{\phi}}$ is the dynamic LTI system in (30).

(b) The mappings $\hat{T}_{e\tilde{\phi}} : \tilde{\phi} \rightarrow e$ and $\Delta : e \rightarrow \tilde{\phi}$ have finite $\mathcal{L}_2$ gains $\gamma(\hat{T}_{e\tilde{\phi}})$ and $\gamma(\Delta)$, and moreover they satisfy $\gamma(\hat{T}_{e\tilde{\phi}})\gamma(\Delta) < 1$.

(c) $\hat{T}_{e\tilde{\phi}}$ and Δ are dissipative with the supply rates $\omega_1 = -e^T e + \gamma(\hat{T}_{e\tilde{\phi}})^2 \tilde{\phi}^T \tilde{\phi}$ and $\omega_2 = -\tilde{\phi}^T \tilde{\phi} + \alpha^2 e^T e$ respectively. We will denote by S_1 and S_2 the corresponding storage functions.

It is a direct application of Corollary 1 in (Hill & Moylan, 1977) (see also (Marquez, 2003), Chapter 9, for a comprehensive review of the subject) that $S_1 + aS_2,\ a > 0$, is a Lyapunov function for this system, and that, since $\gamma(\hat{T}_{e\tilde{\phi}})\gamma(\Delta) < 1$, the system is asymptotically stable. This implies that $e \rightarrow 0$ as $t \rightarrow \infty$.
It also follows that under the same conditions of Theorem 2, if condition (5) holds locally, then local asymptotic convergence of the observer is guaranteed (and in this case the observer (8)-(11) is a local one, i.e, it is local in "x" and in the estimation error "e").
Since the feedback interconnection is asymptotically stable when the measurement error vector $f(t)$ is equal to zero, the residual vector $r(t)$ consequently will converge to zero, and this completes the proof. △

The importance of this theorem is twofold: First, it presents a generalized condition which guarantees observer stability, and hence measurement error detectability, for the new dynamic observer framework. Second, it paves the way for an analytical solution for the design problem, and a design procedure which could easily be implemented using available software packages as will be discussed next.

3.1 An analytical design procedure based on H_∞ regularization

As mentioned earlier, the stability condition in (29) can be represented by the H_∞ norm of the setup in Fig. 1 where G has the state space representation in (14) with appropriate matrices. However, this H_∞ problem does not satisfy all the regularity assumptions in the H_∞ framework (notice that $D_{12}^T D_{12}$ and $D_{21} D_{21}^T$ are both singular). Although the LMI approach in (Iwasaki & Skelton, 1994), or the techniques in (Scherer, 1992); (Stoorvogel, 1996) can be used to solve this singular problem, we here focus on the Riccati approach in (Doyle et al., 1989) by showing that the problem is actually equivalent to the so-called "Simplified H_∞ problem" defined in (Doyle et al., 1989); (Zhou & Doyle, 1998). This helps to directly relate the stability condition to two Riccati equations, instead of the one defined for the static observer framework in (Raghavan & Hedrick, 1994), and lays the ground to a systematic design procedure which is less restrictive than the existing design approaches. This also has the advantage of classifying the set of all possible observer gains by using the standard parameterization of H_∞ controllers in (Doyle et al., 1989); (Zhou & Doyle, 1998). Towards this objective, the following standard regularization procedure is adopted: By replacing the measurement error vector with a "weighted" disturbance term $\epsilon\, d(t)$ ($\epsilon > 0$) in the output equation (4), and using the same observer defined by (21)-(24), it can be seen that the standard H_∞ problem has now the form:

$$\dot{z} = \begin{bmatrix} A \end{bmatrix} z + \begin{bmatrix} \begin{bmatrix} I_n & 0_{np} \end{bmatrix} & -I_n \end{bmatrix} \begin{bmatrix} \begin{bmatrix} \tau \\ d \end{bmatrix} \\ \nu \end{bmatrix} \tag{31}$$

$$\begin{bmatrix} \begin{bmatrix} \zeta \\ \beta\nu \end{bmatrix} \\ \varphi \end{bmatrix} = \begin{bmatrix} \begin{bmatrix} I_n \\ 0_n \end{bmatrix} \\ C \end{bmatrix} z + \begin{bmatrix} \begin{bmatrix} 0_n & 0_{np} \\ 0_n & 0_{np} \end{bmatrix} & \begin{bmatrix} 0_n \\ \beta I_n \end{bmatrix} \\ \begin{bmatrix} 0_{pn} & \epsilon I_p \end{bmatrix} & 0_{pn} \end{bmatrix} \begin{bmatrix} \begin{bmatrix} \tau \\ d \end{bmatrix} \\ \nu \end{bmatrix} \tag{32}$$

which can still be represented by the setup in Fig. 1, by redefining the matrices in (14) and by replacing τ by $\bar{\tau}$ defined as: $\bar{\tau} \stackrel{\Delta}{=} \begin{bmatrix} \tau & d(t) \end{bmatrix}^T$ and ζ by $\bar{\zeta}$ defined as: $\bar{\zeta} = \begin{bmatrix} \zeta & \beta\nu \end{bmatrix}^T$, ($\beta > 0$). It follows that the standard form in (31)-(32) satisfies the conditions of the so-called "*Simplified H_∞ problem*" (Doyle et al., 1989); (Zhou & Doyle, 1998) if and only if (A, C) is detectable, which does not impose any new design restrictions on the observer design. The equivalence between the original problem and this "*Simplified H_∞ problem*" can also be shown as follows: Assume T_1 as the setup in Fig. 1 associated with the original τ and ζ. And assume T_2 as the one associated with $\bar{\tau}$ and $\bar{\zeta}$, i.e the one described by equations (31)-(32). Assume both setups use the observer gain K in (25). And let $\hat{T}_1(s)$ and $\hat{T}_2(s)$ be their corresponding transfer matrices. The following lemma demonstrates certain equivalence relationships among these two setups (the proof of this Lemma is omitted and can be found in (Pertew et al., 2005)).

Lemma 1. *Given the same observer gain controller K for the setups T_1 and T_2 defined above, then $\| \hat{T}_1(s) \|_\infty < \gamma$ if and only if $\exists\, \epsilon > 0, \beta > 0$ such that $\| \hat{T}_2(s) \|_\infty < \gamma$.*

This now lays the ground to the main result of this section, in the form of a theorem showing that the observer gain K needed to stabilize the observer error dynamics and achieve measurement error detection according to Theorem 2 must solve a "*Simplified H_∞ control problem*" according to the definition used in (Zhou & Doyle, 1998). To this end, we define the "Nonlinear Lipschitz observer design problem" as follows:

Definition 5. *(Nonlinear Lipschitz observer design problem) Given $\epsilon > 0$ and $\beta > 0$, find $\mathcal{S}$, the set of admissible observer gains K satisfying $\| \hat{T}_{\bar{\zeta}\bar{\tau}} \|_\infty < \frac{1}{\alpha}$ for the setup in Fig. 1 with G having the state space representation in (14) along with the matrices in (31)-(32).*

Defining the following two Hamiltonian matrices associated with this problem:

$$N_\infty = \begin{bmatrix} A & \alpha^2 I_n - \frac{1}{\beta^2} I_n \\ -I_n & -A^T \end{bmatrix}, \quad J_\infty = \begin{bmatrix} A^T & \alpha^2 I_n - \frac{1}{\epsilon^2} C^T C \\ -I_n & -A \end{bmatrix} \tag{33}$$

the main result is then summarized as follows:

Theorem 3. *There exists a dynamic observer gain K for the observer (8)-(11) (or a static gain L for the classical observer in (6)-(7)) that achieves measurement error detection according to Theorem 2 if and only if $\exists\, \epsilon,\ \beta > 0$ such that:*
1) $N_\infty \in\ dom(Ric)$ and $X_\infty = Ric(N_\infty) > 0$.
2) $J_\infty \in\ dom(Ric)$ and $Y_\infty = Ric(J_\infty) > 0$.
3) $\rho(X_\infty Y_\infty) < \frac{1}{\alpha^2}$ (where $\rho(.)$ is the spectral radius).

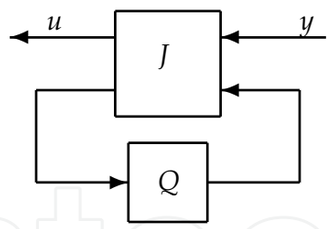

$$\hat{J}(s) = \left[\begin{array}{c|cc} \hat{A}_\infty & \frac{1}{\epsilon^2}(I_n - \alpha^2 Y_\infty X_\infty)^{-1} Y_\infty C^T & -\frac{1}{\beta}(I_n - \alpha^2 Y_\infty X_\infty)^{-1} \\ \hline \frac{1}{\beta^2} X_\infty & 0_{np} & \frac{1}{\beta} I_n \\ -\frac{1}{\epsilon} C & \frac{1}{\epsilon} I_p & 0_{pn} \end{array}\right]$$

Fig. 3. Parametrization of all observer gains.

Proof: A direct result of Theorem 2 and Lemma 1. △

Moreover, by using the result in (Doyle et al., 1989), the set of all observer gains K can be represented by the set of all transfer matrices from y to u in Fig. 3:
where $\hat{A}_\infty = A + (\alpha^2 - \frac{1}{\beta^2})X_\infty - \frac{1}{\epsilon^2}(I_n - \alpha^2 Y_\infty X_\infty)^{-1} Y_\infty C^T C$, and Q is such that $\|Q\|_\infty < \frac{1}{\alpha}$.
Based on the previous results, the following iterative "binary search" procedure is proposed to evaluate the observer gain:

Design Procedure:
Step 1 Set $\epsilon, \beta > 0$.
Step 2 Test solvability of the problem in Definition 5 . If the test fails then go to Step 3 ; otherwise solve the problem (using available software packages or using the analytical result of Theorem 3) and any $K \in \mathcal{S}$ (the set of admissible observer gains) is a candidate observer gain that stabilizes the error dynamics and achieves measurement error detection.
Step 3 Set $\epsilon \leftarrow \frac{\epsilon}{2}$, $\beta \leftarrow \frac{\beta}{2}$. If ϵ or $\beta < r$, a threshold value, then *stop* ; otherwise go to Step 2.

Remarks:

- This design procedure is less restrictive than the designs introduced in (Raghavan & Hedrick, 1994); (Rajamani, 1998); (Rajamani & Cho, 1998); (Aboky et al., 2002), since it is directly related to the stability condition through the result of Theorem 3.
- If the H_∞ problem can not be solved due to its infeasibility or due to the software limitations, one can decrease the Lipschitz constant α and this decreases the region of convergence if α is obtained through linearization but is still a possible way to solve the problem. The word *stop* in step 3 can then be replaced by: *decrease α and go to Step 1*. The algorithm is then guaranteed to work as $\alpha \to 0$. The choice of the threshold in step 3 is also important to avoid numerical instability of the used software.
- Design of the H_∞ observer can also be done by including appropriate weightings to emphasize the performance requirements of the observer over specific frequency ranges.
- If some states are not affected by nonlinearities (i.e, if some entries of the Lipschitz function Φ are zeros), the corresponding 1's of the Identity matrix in the matrix B_1 of the setup (31)-(32) can be replaced by zeros. As long as (A, B_1) is controllable, and the

regularity assumptions are satisfied, the observer design is still equivalent to a "*Simplified H_∞ problem*".

4. The Measurement Error Identification Problem

After solving the measurement error detection problem in Section 3, it would be interesting if those results are extended to the identification problem, where the objective of estimating the error magnitudes and locating the error sources are also considered. The advantage of the dynamic formulation is clear at this point: the measurement error detection condition (29) (in Theorem 2) is satisfied by a family of observers, which helps to include the "identification" objective according to Definition 3 as an additional objective.
Since the residual "r" is given by equation (27), it is clear that the observer estimation error "e" constitutes a part of the residual response, and that by minimizing "e" the residual converges to "f" which guarantees measurement error identification in this case. This could be seen by noting that the estimation error "e" can be represented by the feedback interconnection in Fig. 4 where "f" is the measurement error vector that affects the system (compare this representation to the loop dynamics in Fig. 2 when the measurement error vector "f" is equal to zero).

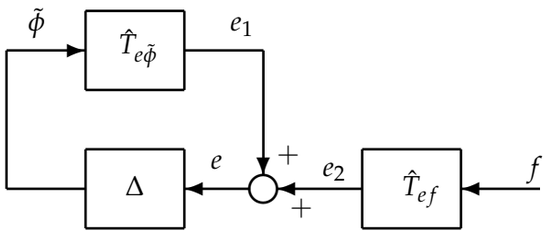

Fig. 4. Observer dynamics with measurement errors.

Therefore, minimizing "e" is equivalent to minimizing the effect of "f" on the feedback interconnection of Fig. 4. This minimization problem can be considered in $\mathcal{L}_2$ sense by assuming the measurement error to have finite energy, and applying the small gain theorem to Fig. 4. This assumption is with no loss of generality, since it is guaranteed over any finite time operation of the observer. In this section, the solution of this minimization problem is considered when "f" is in a narrow frequency band around a nominal frequency ω_o. From the special cases of interest is the case of sensor bias and the case of measurement errors of known harmonics. We first show that the problem is not tractable for the classical structure in (6)-(7), and then present a solution using the dynamic observer. Towards that goal, we will first assume that the Fourier transform of the measurement error $F(j\omega)$ have a frequency pattern restricted to the narrow band $\omega_o \pm \Delta\omega$ as described by equation (34).

$$|F(j\omega)| \leq \begin{cases} A\,; & |\omega - \omega_o| < \Delta\omega \\ \delta\,; & \text{otherwise} \end{cases} \tag{34}$$

where δ is a small neglected number for the frequency magnitudes outside the region of interest, and where A is a positive upper bound on these magnitudes inside the considered domain. We will then define an observer gain K as optimal if $\| e \|_{\mathcal{L}_2}$ can be made

arbitrarily small for all possible measurement errors satisfying (34). But by applying the small gain theorem to Fig. 4 when measurement error detection is satisfied (i.e, when K satisfies $\| \hat{T}_{e\tilde{\phi}} \|_\infty = \mu < \frac{1}{\alpha}$) we have: $\|e\|_{\mathcal{L}_2} \leq \frac{1}{1-\mu\alpha} \|e_2\|_{\mathcal{L}_2}$. And since (as $\Delta\omega \to 0$), $\hat{T}_{ef}(j\omega) \to \hat{T}_{ef}(j\omega_o)$ then we have $\|e_2\|_{\mathcal{L}_2} \leq \sigma_{max}\left(\hat{T}_{ef}(j\omega_o)\right) \|f\|_{\mathcal{L}_2}$, and therefore, it is easy to see that an optimal gain K is one that satisfies $\hat{T}_{ef}(j\omega_o) = 0$. By assuming that the measurement error detection objective is satisfied (as stated in Theorem 2, it follows that *measurement error identification* according to Definition 3 is satisfied if the following two conditions are satisfied: (i) $\| \hat{T}_{e\tilde{\phi}} \|_\infty < \frac{1}{\alpha}$, (ii) $\hat{T}_{ef}(j\omega_o) = 0$, where the first one is a sufficient condition in order to achieve *measurement error detection* according to Definition 1.
Moreover, to include the effect of measurement errors on the standard setup which was used in conjunction with the H_∞ problem in Section 3, the vectors of the setup of Fig. 1 are redefined as: $\tau \triangleq \begin{bmatrix} \tau_1 \\ \tau_2 \end{bmatrix} = \begin{bmatrix} \tilde{\phi} \\ f \end{bmatrix}$, $\nu = \eta$, $\zeta = e$, $\varphi = r$. The residual can be then represented by:

$$\dot{z} = [A]\, z + \begin{bmatrix} [I_n & 0_{np}] & -I_n \end{bmatrix} \begin{bmatrix} \tau \\ \nu \end{bmatrix} \tag{35}$$

$$\begin{bmatrix} \zeta \\ \varphi \end{bmatrix} = \begin{bmatrix} I_n \\ C \end{bmatrix} z + \begin{bmatrix} [0_n & 0_{np}] & 0_n \\ [0_{pn} & I_p] & 0_{pn} \end{bmatrix} \begin{bmatrix} \tau \\ \nu \end{bmatrix} \tag{36}$$

which can also be represented by the standard form in Fig. 1 where G has the representation in (14) with the matrices in (35)-(36) and where K is the dynamic observer gain.
Based on the previous discussion, we define an optimal residual generator as:

Definition 6. *(Optimal residual generator for narrow frequency band) An observer of the form (8)-(12) is said to be an optimal residual generator for the measurement error identification problem (with measurement errors in a narrow frequency band around ω_o) if the observer gain K satisfies $\| \hat{T}_{e\tilde{\phi}} \|_\infty < \frac{1}{\alpha}$ and $\hat{T}_{ef}(j\omega_o) = 0$, for the standard setup in Fig. 1 where the plant G has the state space representation in (14) with the matrices defined in (35)-(36).*

The main result of this section is now presented in the form of a theorem showing that the classical observer structure in (6)-(7) can never be an optimal residual generator. This shows the importance of having a dynamic observer gain in this case.

Theorem 4. *An observer of the form (6)-(7) with a static observer gain L can never be an optimal residual generator according to Definition 6.*

Proof: First, using (35)-(36) and the dynamic observer gain K it can be shown that $\hat{T}_{ef}$ is given from:

$$T_{ef} = T_{\zeta\tau_2} = \left[\begin{array}{cc|c} A - D_L C & -C_L & -D_L \\ B_L C & A_L & B_L \\ \hline I_n & 0_{nk} & 0_{np} \end{array}\right] \tag{37}$$

The proof follows by noting that (when the observer gain K is replaced by the static gain L) the transfer matrix from f to e in (37) is given by $T_{ef} = \left[\begin{array}{c|c} A - LC & -L \\ \hline I_n & 0_{np} \end{array}\right]$. Since the gain L is chosen to stabilize $(A - LC)$, then $(\forall\omega_o)$ $j\omega_o$ is not an eigenvalue of $(A - LC)$. Therefore, by using (13), we have: rank $\left(\hat{T}_{ef}(j\omega_o)\right)$ =rank $\begin{bmatrix} A - LC - j\omega_o I_n & -L \\ I_n & 0_{np} \end{bmatrix} - n$. But

$\text{rank}\begin{bmatrix} A-LC-j\omega_o I_n & -L \\ I_n & 0_{np} \end{bmatrix} = \text{rank}\begin{bmatrix} 0_n & L \\ I_n & 0_{np} \end{bmatrix} = n + \text{rank}(L)$ (using the invariant zero property (13)).

Therefore, $\text{rank}\left(\hat{T}_{ef}(j\omega_o)\right) \neq 0$ unless $L = 0$. This implies that no gain L can satisfy $\hat{T}_{ef}(j\omega_o) = 0$, and therefore the static observer structure can never be an optimal residual generator according to Definition 6. △

In the following section (section 4.1), a numerical approach based on LMIs is provided, by modelling the problem as a convex optimization problem using the dynamic observer structure in (8)-(12).

4.1 A LMI Design Procedure

The second objective, i.e $\hat{T}_{ef}(j\omega_o) = 0$, can also be modelled as a weighted H_∞ problem solvable using the dynamic observer formulation. To this end, we first note that for an observer gain K that satisfies the measurement error detection condition (as stated in Theorem 2, the following two statements are equivalent: (i) $\hat{T}_{ef}(j\omega_o) = 0$, (ii) $W(s)\hat{T}_{ef}(s) \in RH_\infty$, where $W(s) = diag_p(\frac{1}{s})$ if $\omega_o = 0$ and $W(s) = diag_p(\frac{1}{s^2+\omega_o^2})$ if $\omega_o \neq 0$. The equivalence of these two statements can be seen by first noting that the condition in Theorem 2 implies that $\| \hat{T}_{e\tilde{\phi}} \|_\infty < \frac{1}{\alpha}$ and hence that $\hat{T}_{e\tilde{\phi}} \in RH_\infty$. It then follows that $\hat{T}_{ef}(s) \in RH_\infty$ since T_{ef} in (37) and $T_{e\tilde{\phi}}$ both have the same state transition matrix. Finally, since $\hat{T}_{ef}(j\omega_o) = 0$ corresponds to $j\omega_o$ being a system zero of $\hat{T}_{ef}(s)$ (which is equivalent to cancelling the poles of $W(s)$ on the imaginary axis), it follows that $\hat{T}_{ef}(j\omega_o) = 0$ is equivalent to having $W(s)\hat{T}_{ef}(s) \in RH_\infty$.

According to the previous discussion, it follows that the objective $\hat{T}_{ef}(j\omega_o) = 0$ can be restated as follows: $\exists \epsilon > 0$ such that $\left\{ \epsilon \parallel W(s)\hat{T}_{ef}(s) \parallel_\infty < \frac{1}{\alpha} \right\}$, where the scalar "$\epsilon$" is used for compatibility with the first objective (i.e, $\| \hat{T}_{e\tilde{\phi}} \|_\infty < \frac{1}{\alpha}$). The two objectives can then be combined in the unified framework in Fig. 5, where the plant G has the state space representation in (14) with the matrices defined in (35)-(36).

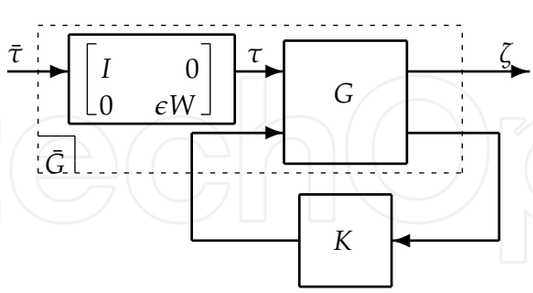

Fig. 5. Weighted standard setup.

It can be seen that the augmented plant $\bar{G}$ in Fig. 5 is given by:

$$\bar{G} = \left[\begin{array}{c|cc} \bar{A} & \bar{B}_1 & \bar{B}_2 \\ \hline \bar{C}_1 & \bar{D}_{11} & \bar{D}_{12} \\ \bar{C}_2 & \bar{D}_{21} & \bar{D}_{22} \end{array}\right] = \left[\begin{array}{c|cc} \begin{bmatrix} A_\theta & 0_{\ell n} \\ 0_{n\ell} & A \end{bmatrix} & \begin{bmatrix} 0_{\ell n} & B_\theta \\ I_n & 0_{np} \end{bmatrix} & \begin{bmatrix} 0_{\ell n} \\ -I_n \end{bmatrix} \\ \hline \begin{bmatrix} 0_{n\ell} & I_n \\ \epsilon C_\theta & C \end{bmatrix} & \begin{bmatrix} 0_n & 0_{np} \\ 0_{pn} & 0_p \end{bmatrix} & \begin{bmatrix} 0_n \\ 0_{pn} \end{bmatrix} \end{array}\right] \tag{38}$$

where:

$$\begin{cases} \ell = p,\ A_\theta = 0_p,\ B_\theta = I_p,\ C_\theta = I_p\ ;\ \text{if } \omega_o = 0 \\ \ell = 2p,\ A_\theta = diag_p \begin{bmatrix} 0 & 1 \\ -\omega_o^2 & 0 \end{bmatrix},\ B_\theta = diag_p \begin{bmatrix} 0 \\ 1 \end{bmatrix},\ C_\theta = diag_p \begin{bmatrix} 1 & 0 \end{bmatrix};\ \text{if } \omega_o \neq 0 \end{cases} \tag{39}$$

The following theorem gives necessary and sufficient conditions for solving the measurement error identification problem in Definition 6:

Theorem 5. *Given the system (3)-(4), there exists an optimal residual according to Definition 6,* $\forall\ \Phi$ *satisfying (5) with a Lipschitz constant* α*, if and only if* $\exists\ \epsilon > 0$ *and a dynamic observer gain K satisfying* $\| \hat{T}_{\zeta\bar{\tau}} \|_\infty < \frac{1}{\alpha}$.

Proof: A direct result of Definition 6 and the discussion in the beginning of Section 4.1 showing the equivalence between the two objectives. △

However, standard H_∞ tools can not be directly applied for the H_∞ problem defined in Theorem 5, unlike the measurement error detection problem discussed in Section 3. For instance the Riccati approach in (Zhou & Doyle, 1998) can not be implemented since the augmented plant $\bar{G}$ in (38) does not satisfy the needed regularity assumptions. Also, the LMIs in equation (15)-(17) are not feasible due to the poles that $\bar{G}$ has on the imaginary axis, making the use of the LMI approach in (Gahinet & Apkarian, 1994) impossible. However, by replacing the weightings $W(s)$ by the modified weightings $\bar{W}(s)$ where $\bar{W}(s) = diag_p(\frac{1}{s+\lambda})$ if $\omega_o = 0$ and $\bar{W}(s) = diag_p(\frac{1}{s^2+2\lambda\omega_o s+\omega_o^2})$ if $\omega_o \neq 0$, with $\lambda \in \mathbb{R}^+$, the augmented plant $\bar{G}$ in Fig. 5 is still given by equation (38), but with A_θ as:

$$A_\theta = \begin{cases} diag_p(-\lambda) \quad ; & \omega_o = 0 \\ diag_p \begin{bmatrix} 0 & 1 \\ -\omega_o^2 & -2\lambda\omega_o \end{bmatrix}; & \omega_o \neq 0 \end{cases} \tag{40}$$

which has no poles on the imaginary axis. Using the modified plant and the result in Theorem 1, the following convex optimization problem is proposed to solve the problem in Theorem 5:

$$\begin{aligned} &min_{R,S}\ \lambda \\ &\text{subject to " the 3 LMIs in (15)-(17) with } \gamma = \frac{1}{\alpha} \text{ "} \end{aligned}$$

with the matrices in (15)-(17) replaced by the corresponding ones in (38)-(40).

The set of all admissible observer gains K for a given λ can then be parameterized using R, S by using the result in (Gahinet & Apkarian, 1994). It can also be seen, that these LMIs are feasible for all $\lambda > 0$, and that minimizing λ in this case is equivalent to minimizing $\sigma_{max}\left(\hat{T}_{ef}(j\omega_o)\right)$. This guarantees that the proposed optimization problem converges to the existing solution as $\lambda \to 0$. It also guarantees that standard software packages can be used to solve this optimization problem.

The optimal residual generator guarantees measurement errors estimation and at the same time state estimation. An advantage of having *state* estimation in the presence of measurement errors is the possibility to use the observer in fault tolerant output feedback control (i.e, if a reconfiguration control action is involved). Also, from the special cases of interest is the case of sensor bias, where the previous approach can be used to get an *exact* estimation of all sensor biases at the same time. An important advantage over the adaptive approaches used to

diagnose sensor biases in nonlinear systems, such as (Vemuri, 2001); (Wang et al., 1997), is the ability to diagnose piecewise constant bias with the same observer. Moreover, the proposed approach is not limited to sensor biases and can be used to diagnose measurement errors of any harmonics.

5. Measurement Error Identification for Low and High Frequencies

We now consider measurement errors of low frequencies determined by a cutoff frequency ω_l. The SISO weighting $\hat{w}_l(s) = \frac{as+b}{s}$, (Zhou & Doyle, 1998), emphasizes this range with "b" selected as ω_l and "a" as an arbitrary small number for the magnitude of $\hat{w}_l(j\omega)$ as $\omega \to \infty$. With a diagonal transfer matrix $\hat{W}(s)$ that consists of these SISO weightings (and similar to the approach adopted in section 4.1), the detection and identification objectives can be combined in the unified framework represented by the weighted setup of Fig. 5. In this case, the augmented plant $\bar{G}$ is given by:

$$\bar{G} = \left[\begin{array}{c|cc} \bar{A} & \bar{B}_1 & \bar{B}_2 \\ \hline \bar{C}_1 & \bar{D}_{11} & \bar{D}_{12} \\ \bar{C}_2 & \bar{D}_{21} & \bar{D}_{22} \end{array}\right] = \left[\begin{array}{c|c|c} \begin{bmatrix} A_\theta & 0_{pn} \\ 0_{np} & A \end{bmatrix} & \begin{bmatrix} 0_{pn} & B_\theta \\ I_n & 0_{np} \end{bmatrix} & \begin{bmatrix} 0_{pn} \\ -I_n \end{bmatrix} \\ \hline \begin{bmatrix} 0_{np} & I_n \\ \epsilon C_\theta & C \end{bmatrix} & \begin{bmatrix} 0_n & 0_{np} \\ 0_{pn} & \epsilon D_\theta \end{bmatrix} & \begin{bmatrix} 0_n \\ 0_{pn} \end{bmatrix} \end{array}\right] \tag{41}$$

where A_θ=0_p, B_θ=I_p, C_θ=$diag_p(b)$ and D_θ=$diag_p(a)$. This form also violates the assumptions of Theorem 1 (note that $(\bar{A}, \bar{B}_2)$ is not stabilizable). Similar to Section 4, we introduce the modified weighting $\hat{w}_{lmod}(s)$=$\frac{as+b}{s+\lambda}$; with arbitrary small positive "λ". The augmented plant $\bar{G}$ is then the same as (41) except for A_θ which is now given by the stable matrix $diag_p(-\lambda)$ and C_θ given by $diag_p(b - a\lambda)$. Similar to the narrow frequency band case, the assumptions of Theorem 1 are now satisfied and the LMI approach in (Gahinet & Apkarian, 1994) can be used to solve the H_∞ problem. To this end, we define the H_∞ problem associated with the low frequency range as follows:

Definition 7. *(Low frequency H_∞) Given $\lambda > 0$, $\epsilon > 0$, find $\mathcal{S}$, the set of admissible controllers K satisfying $\| \hat{T}_{\zeta\bar{\tau}} \|_\infty < \gamma$ for the setup in Fig. 5 where $\bar{G}$ has the state space representation (41) with $A_\theta = diag_p(-\lambda)$, $B_\theta = I_p$, $C_\theta = diag_p(b - a\lambda)$ and $D_\theta = diag_p(a)$.*

Based on all the above, we now present the main result of this section in the form of the following definition for an optimal residual generator in $\mathcal{L}_2$ sense:

Definition 8. *(Optimal residual for low frequencies) An observer of the form (8)-(12) is an optimal residual generator for the measurement error identification problem (with low frequency measurement errors below the cutoff frequency ω_l) if the dynamic gain $K \in \mathcal{S}^*$ (the set of controllers solving the H_∞ problem in Definition 7 for $\gamma = 1/\alpha$ with the minimum possible λ).*

Similar to the low frequency range, a proper weighting $\hat{w}_{hmod}(s) = \frac{s+(a\times b)}{\lambda s+b}$, (Zhou & Doyle, 1998), with an arbitrary small $\lambda > 0$, could be selected to emphasize the high frequency range $[w_h, \infty)$ with "b" selected as w_h and "a" as an arbitrary small number for $|\hat{w}_h(j\omega)|$ as $\omega \to 0$. With the help of $\hat{w}_{hmod}(s)$, a suitable weighting W that emphasizes the high frequency range can be designed. The augmented $\bar{G}$ is also given from (41) (same as the low frequency case), but with A_θ, B_θ, C_θ and D_θ given as $diag_p(-\frac{b}{\lambda})$, I_p, $diag_p(\frac{a\times b}{\lambda} - \frac{b}{\lambda^2})$ and $diag_p(\frac{1}{\lambda})$ respectively. It is straightforward that $\bar{G}$ satisfies all of the assumptions of Theorem 1 and therefore, similar to the low frequency range, an H_∞ problem related to the high frequency range can be defined. An optimal residual generator can be defined in the same way as Definition 8 for the generalized low frequency case.

6. Experimental Results

The experimental results presented in this section (Pertew, 2006) are intended to illustrate the applicability of the theoretical results presented in this chapter for robotic systems.

6.1 The ROTPEN: Models and Assumptions

The *Quanser* rotary inverted pendulum (ROTPEN) is shown schematically in Fig. 6, Lynch (2004). The angle that the perfectly rigid link of length l_1 and inertia J_1 makes with the x-axis of an inertial frame is denoted θ_1 (degrees). Also, the angle of the pendulum (of length l_2 and mass m_2) from the z-axis of the inertial frame is denoted θ_2 (degrees).

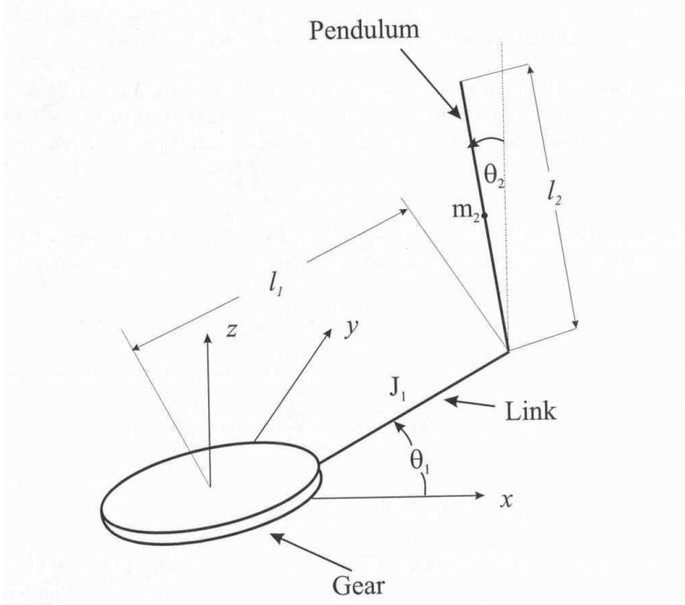

Fig. 6. The Rotary Inverted Pendulum (ROTPEN).

The system has one input which is the scalar servomotor voltage input (Volt). Therefore, the system is a special case of the robot manipulator model discussed in Section 1: a planar robot manipulator with two links ($n = 2$), with only one torque applied at the first joint, while the second joint is subject to the gravitational force. In fact, the ROTPEN has a state space model of the form $\dot{x} = f(x) + g(x)u$, where $x = [\theta_1\ \theta_2\ \dot{\theta_1}\ \dot{\theta_2}]^T$ is the state vector, and u is the scalar servomotor voltage input (Volt). More details about this model and its parameters can be found in Appendix 9.1.

The system has an infinite number of equilibrium points, representing the following two equilibrium points:

1) Pendant position: $x_1 = 0$ (rad), $x_2 = \pi$ (rad), $x_3 = x_4 = 0$ (rad/sec).
2) Inverted position: $x_1 = x_2 = 0$ (rad), $x_3 = x_4 = 0$ (rad/sec).

By separating the nonlinear terms, the model can be put in the form $\dot{x} = Ax + \Phi(x, u)$, where:

$$A = \begin{bmatrix} 0 & 0 & 1 & 0 \\ 0 & 0 & 0 & 1 \\ 0 & -25.14 & -17.22 & 0.2210 \\ 0 & 68.13 & 16.57 & -0.599 \end{bmatrix}, \quad \Phi(x,u) = \begin{bmatrix} 0 \\ 0 \\ \phi_1(x,u) \\ \phi_2(x,u) \end{bmatrix}.$$

The nonlinear terms in Φ are

mainly trigonometric terms, and using the symbolic MATLAB toolbox, an upper bound on $\|\Phi(x,u)\|$ is found as 44.45, and hence the Lipschitz constant for the ROTPEN is $\alpha = 44.45$. This follows from the fact that if $\Phi : \mathbb{R}^n \times \mathbb{R} \to \mathbb{R}^m$ is continuously differentiable on a domain D and the derivative of Φ with respect to the first argument satisfies $\|\frac{\partial \Phi}{\partial x}\| \leq \alpha$ on D, then Φ is Lipschitz continuous on D with constant α, i.e.:

$$\|\Phi(x,u) - \Phi(y,u)\| \leq \alpha \|x - y\|, \forall\, x,\, y \in D \tag{42}$$

There are two encoders to measure the angle of the servomotor output shaft (θ_1) and the angle of the pendulum (θ_2). An encoder is also available to measure the motor velocity $\dot{\theta_1}$, but no one is available to measure the pendulum velocity $\dot{\theta_2}$. In the experiments, linear as well as nonlinear control schemes are used to stabilize the pendulum at the inverted position ($\theta_2 = 0$), while tracking a step input of 30 degrees for the motor angle.

6.2 Case Study 1 - Lipschitz Observer Design

In this experiment, we focus on the nonlinear state estimation problem when no measurement errors are affecting the system. We consider situations in which the operating range of the pendulum is either close or far from the equilibrium point, comparing the Luenberger observer with the Lipschitz observer in these cases. For the purpose of applying the Lipschitz observer design, the nonlinear model discussed in section 6.1 is used. We also compare the dynamic Lipschitz observer of section 3 with the static design method in Reference (Raghavan & Hedrick, 1994). In this case study the full-order linear and Lipschitz models are used for observer design, where the output is assumed as $y = [x_1 \;\; x_2]^T$ (all the observer parameters that are used in this experiment can be found in Appendix 9.2).
First, a linear state feedback controller is used to stabilize the system in a small operating range around the inverted position, and three observers are compared:

1) Observer 1: A linear Luenberger observer where the observer gain is obtained by placing the poles of $(A - LC)$ at $\{-24, \;\; -3.8, \;\; -4.8, \;\; -12.8\}$ (see $L_{3-small}$ in Appendix 9.2).
2) Observer 2: A high gain Luenberger observer, which has the same form of Observer 1 but with the poles placed at $\{-200, \;\; -70, \;\; -20 + 15i, \;\; -20 - 15i\}$ (see $L_{3-large}$ in Appendix 9.2).
3) Observer 3: A Lipschitz observer of the form (8)-(11), based on the full-order Lipschitz model of the ROTPEN. The dynamic gain is computed using the design procedure in section 3.1, for $\alpha = 44.45$ (see K_3 in Appendix 9.2).

The three observers run successfully with stable estimation errors. Table 1 shows the maximum estimation errors in this case. It can be seen that both the Luenberger observer (large poles) and the Lipschitz observer achieve comparable performance, which is much better than the Luenberger observer with small poles. The three observers are also tested in observer-based control, and their tracking performance is compared in Table 2. We conclude that, due to the small operating range considered in this case study, a high-gain Luenberger observer achieves a good performance in terms of the state estimation errors and the tracking errors.
We then consider a large operating range by using a nonlinear control scheme that stabilizes the pendulum angle at the pendant position (see Appendix 9.2 for more details about the controller used in this case study). Using this controller, a large operating range is obtained as seen in Fig. 7. The same observers (Observers 2 and 3) are used in parallel with this control scheme, and the resulting estimation errors are compared in Fig. 8. The two observers are also

	Small-gain Luenberger	High-gain Luenberger	Lipschitz
$max\ \|e_1\|$	3.6485	0.4323	0.1716
$max\ \|e_2\|$	1.5681	0.0925	0.1865

Table 1. Case study 1 - Estimation errors "e_1" and "e_2" in degrees

	pure state feedback	High-gain Luenberger	Lipschitz
Percentage of overshoot	20.3613%	12.7440%	48.4863%
$\|$*steady state error*$\|$	2.5635	3.4424	3.7939

Table 2. Case study 1 - Tracking performance in degrees

compared in observer-based control, and the Luenberger observer fails in this case, causing total system unstability. The Lipschitz observer, on the other hand, runs successfully and its performance (compared to the pure state feedback control) is shown in Fig. 9. This case study illustrates the importance of the Lipschitz observer in large operating regions, where the linear observer normally fails.

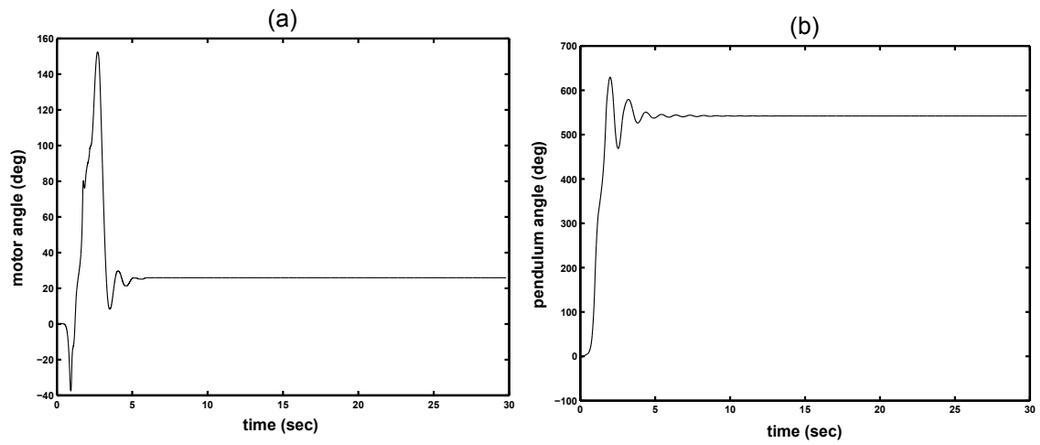

Fig. 7. Case Study 1 - (a) Motor Response, (b) Pendulum Response.

Finally, we conduct a comparison between static and dynamic Lipschitz observers, namely the observer (6)-(7) and the one in (8)-(11). The comparison is between the new design proposed in Section 3 and the one in Reference (Raghavan & Hedrick, 1994). First, the design algorithm in (Raghavan & Hedrick, 1994) is tested for different values of α and ε. It fails for all values of $\alpha > 1$, and the maximum attainable value is $\alpha = 1$ (see L_5 in Appendix 9.2), while the Lipschitz constant of the ROTPEN model is 44.45 as mentioned earlier. This observer is then compared to the dynamic Lipschitz observer having the dynamic gain K_3, and the estimation errors are shown in Fig. 10. It is also important to note that the static Lipschitz observer fails in stabilizing the system, when used in observer-based control, for both the small and large operating range experiments. This shows the importance of the dynamic Lipschitz observer design in this case.

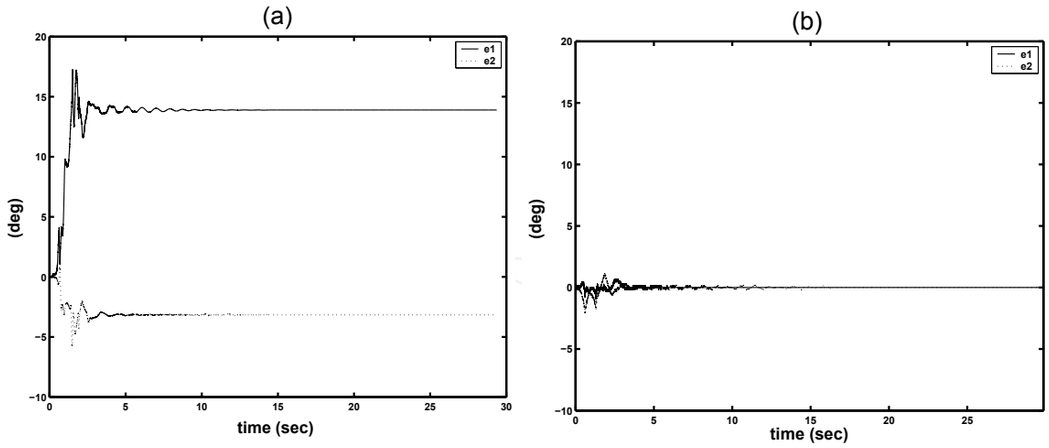

Fig. 8. Case Study 1 - (a) High-gain Luenberger Errors, (b) Dynamic Lipschitz Errors.

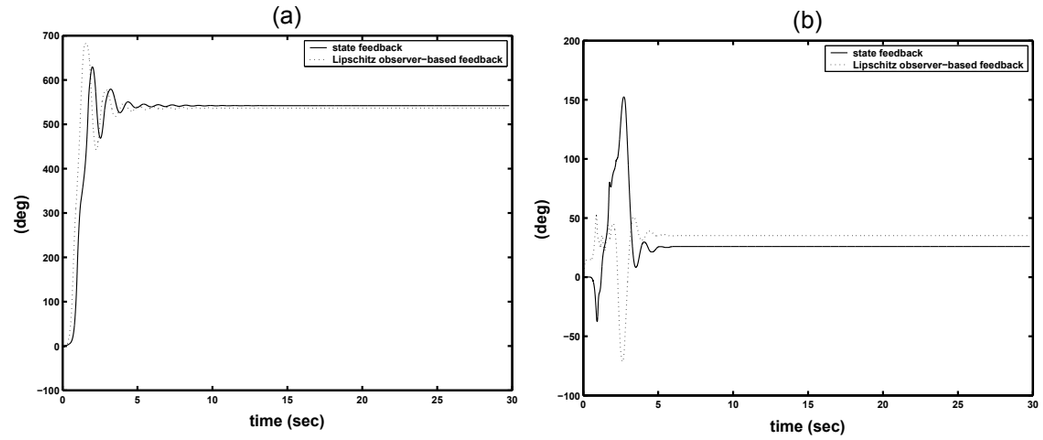

Fig. 9. Case Study 1 - (a) Pendulum Angle, (b) Motor Angle.

6.3 Case Study 2 - Lipschitz Measurement Error Diagnosis

In this experiment, the results of Sections 4 and 5 are assessed on the nonlinear Lipschitz model. A large operating range is considered by using a nonlinear, switching, LQR control scheme (with integrator) that stabilizes the pendulum at the inverted position (starting from the pendant position) while tracking a step input of 30 degrees for the motor angle as seen in Fig. 11 (the no-bias case). In the first part of this experiment, an important measurement error that affects the ROTPEN in real-time is considered. This is a sensor fault introduced by the pendulum encoder. The encoder returns the pendulum angle relative to the initial condition, assuming this initial condition to be $\theta_2 = 0$. This constitutes a source of bias, as shown in Fig. 11(b), when the pendulum initial condition is unknown or is deviated from the inverted position. The effect of this measurement error on the tracking performance is also illustrated in Fig. 11(a) for two different bias situations. The dynamic Lipschitz observer (discussed in section 4) is applied to diagnose and tolerate this fault. In addition to this bias fault, the observer is also applied for a 2 rad/sec fault introduced in real-time, as well as for the case of a low frequency fault in the range $[0, 1$ rad/sec$]$.

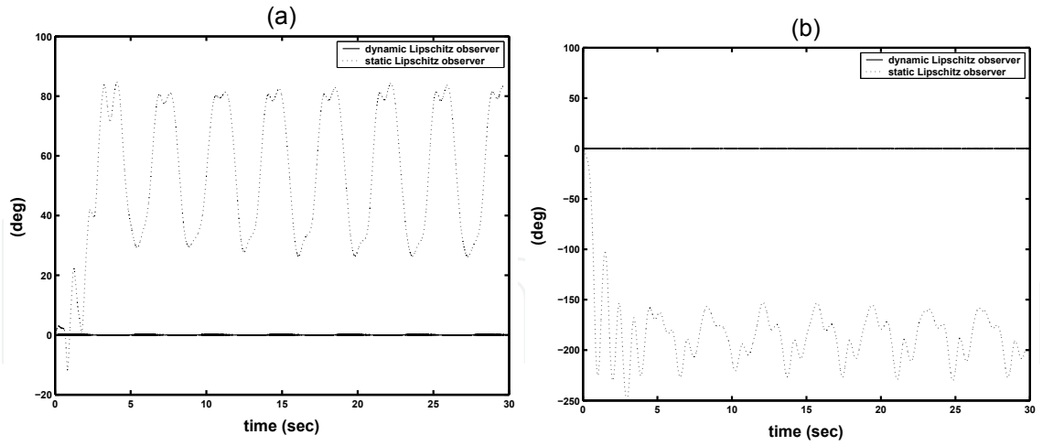

Fig. 10. Case Study 1 - (a) Estimation Error "e_1", (b) Estimation Error "e_2".

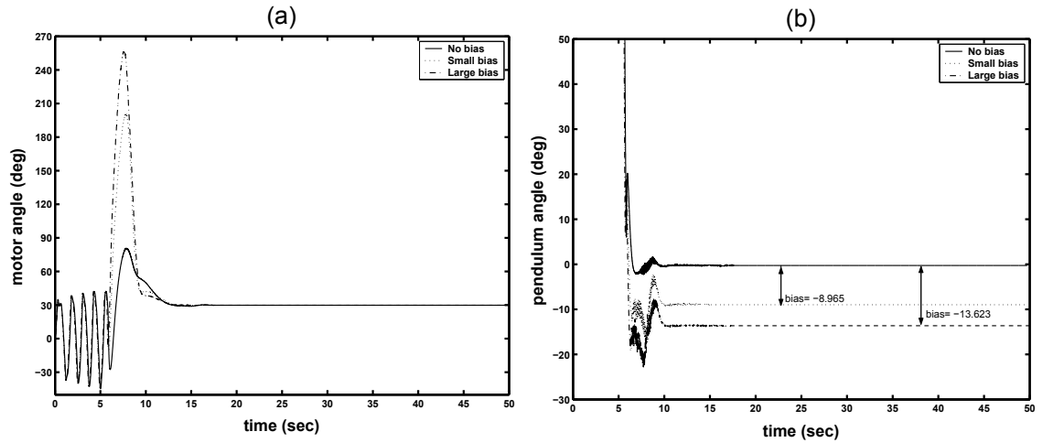

Fig. 11. Case Study 2 - (a) Tracking Performance, (b) Pendulum Angle.

First, the design procedure in section 4 is used to accurately estimate and tolerate the bias faults shown in Fig. 11(b). This is the special case where $\omega_o = 0$. Using the reduced-order Lipschitz model with $\alpha = 44.45$ (and using the LMI design procedure, the dynamic gain for the observer (8)-(12) that achieves measurement error identification is obtained as K_6 (see Appendix 9.3 for more details). Using this observer, the biases affecting the system in Fig. 11 are successfully estimated as shown in Fig. 12. Moreover, by using this observer in an observer-based control scheme, the tracking performance in the large bias case is illustrated in Fig. 13. The performance is much improved over the one with no fault tolerance as seen in Fig. 13(b). It also gives less overshoot than the no bias case, as seen in Fig. 13(a). Similar results are obtained for the small bias case.

The case of measurement error in the form of harmonics is now considered, with a sensor fault having a frequency of 2 rad/sec. The dynamic gain for the observer (8)-(12) is computed using the design approach discussed in section 5. This is the special case where $\omega_o = 2$. The gain is obtained at $\lambda = 10^{-12}$ as K_7 (see Appendix 9.3). Using this observer, Fig. 14 shows the correct estimation of a measurement error of amplitude 20 degrees and frequency 2 rad/sec.

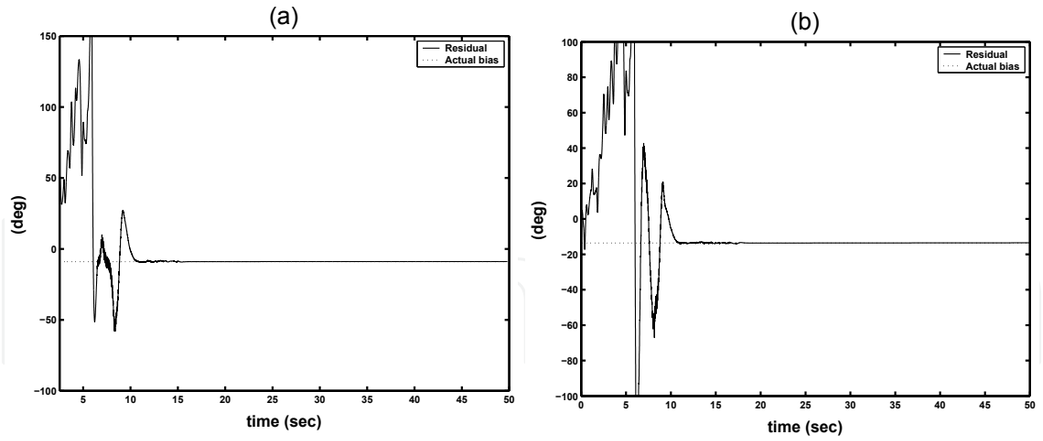

Fig. 12. Case Study 2 - (a) Estimation of the Small Bias, (b) Estimation of the Large Bias.

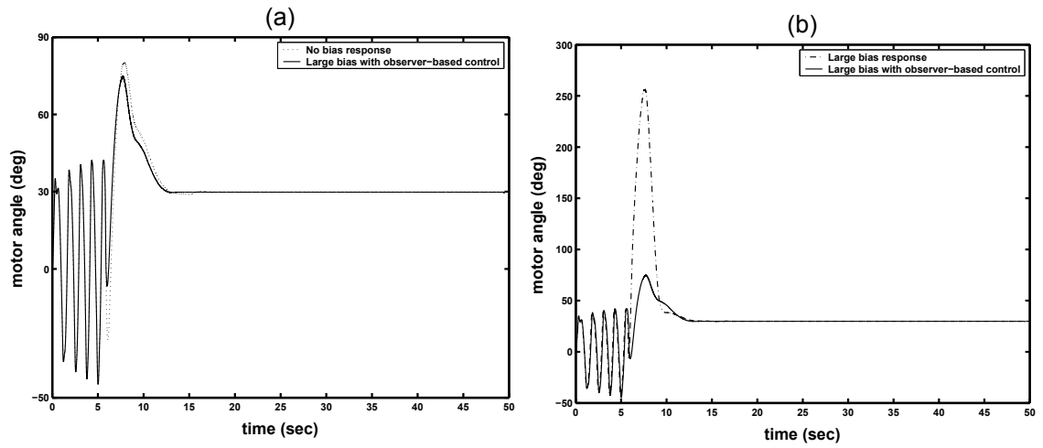

Fig. 13. Case Study 2 - (a) No-bias versus Observer-based, (b) Large Bias versus Observer-based.

We then consider the case of low frequency sensor faults (in the range $[0,\ 1\ \text{rad/sec}]$). Using the design introduced in section 5 (and with $a = 0.1$, $b = 1$ and $\epsilon = 0.1$), the optimal observer gain is obtained using the command *hinflmi* in MATLAB, with minimum λ as 10^{-12} (see K_8 in Appendix 9.3). Using this observer for measurement error diagnosis, a correct estimation of a low frequency sensor fault (generated using the MATLAB command *idinput*) is shown in Fig. 15.

7. Conclusion

The Lipschitz observer design approach provides an important framework for solving the measurement error diagnosis problem in robot manipulators. The classical observer structure is not directly applicable to the detection and identification problems. This is in part due to the restrictive observer structure, and also due to the idealized assumptions inherent in this structure that do not take into account uncertain model parameters and disturbances. The dynamic observer structure offers two important advantages in that regard: (i) The observer stability condition that ensures asymptotic convergence of the state estimates is satisfied by a family

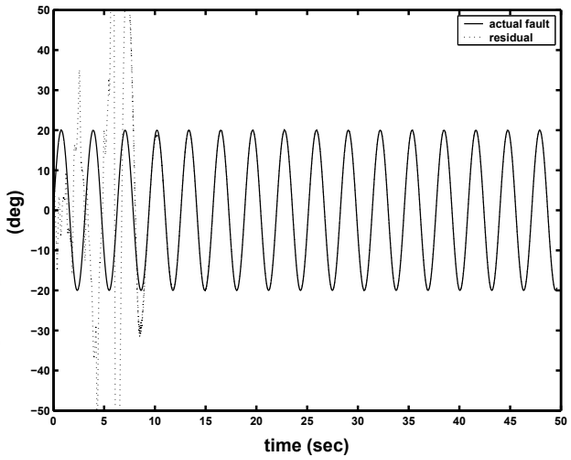

Fig. 14. Case Study 2 - Frequency Band Estimation.

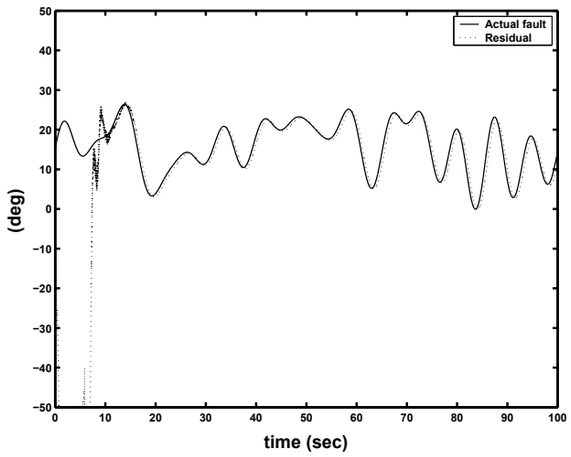

Fig. 15. Case Study 2 - Diagnosis of Low Frequency Sensor Fault.

of observers, adding extra degrees of freedom to the observer which lay the ground to the addition of the detection and identification objectives in the design, (ii) The observer design can be carried out using a systematic design procedure which is less restrictive than the existing design approaches and which is solvable using commercially available software. The design depends heavily on the nature of the objectives considered. While an analytical solution can be used for measurement error detection, the identification problem is more demanding and needs a more general design framework. This problem is shown to be equivalent to a standard convex optimization problem which is solvable using Linear Matrix Inequalities (LMIs). Using this generalized framework, different frequency patterns for the measurement errors that affect the robot manipulator could be considered, and systematic design procedures could be used to solve the problem. A practical example, namely the *Quanser* rotary inverted pendulum (ROTPEN) in the Control Systems Lab, Electrical and Computer Engineering department, University of Alberta, is used to illustrate these results. The ROTPEN model falls in the category of planar robot manipulators, and the experimental results illustrate the applicability of the proposed techniques in the robotics field by showing the following:

i) How to model a robot manipulator as a standard Lipschitz system.

ii) The importance of the dynamic Lipschitz observer in large operating regions where the linear observer normally fails.

iii) The accurate velocity estimations obtained using the dynamic observer, alleviating the need to introduce velocity sensors in real-time.

iv) How the static observer fails, compared to the dynamic observer, when applied to Robotic Systems due to the large Lipschitz constant that these systems normally have.

v) The efficiency of the dynamic observer in diagnosing and tolerating measurement errors of different frequencies, including an important bias introduced by the error in the initial conditions of the pendulum encoder.

8. Acknowledgement

The author would like to thank the Advanced Control Systems Laboratory members at University of Alberta. Special thanks to Dr. Alan Lynch and to Dr. Thomas Grochmal for providing the ROTPEN equations and the switching swingup control scheme used in the experiments.

9. Appendix

9.1 The ROTPEN Model

The system parameters are: $l_1 = 0.215$ m, $l_2 = 0.335$ m, $m_2 = 0.1246$ Kg, $\beta = 0.135 Nm/s$, $\mu = 0.2065 Nm/V$, $b_2 = 0.0018 Kg/s$, $g = 9.81 m/s^2$, and $J_1 = 0.0064$ Kg.m^2. With the state defined as $x = [x_1\ x_2\ x_3\ x_4]^T = [\theta_1(\text{rad})\ \theta_2(\text{rad})\ \dot{\theta_1}(\text{rad/s})\ \dot{\theta_2}(\text{rad/s})]^T$, the state space model has the form $\dot{x} = f(x) + g(x)u$ as follows (This model was derived in Lynch (2004)):

$$\dot{x} = \begin{bmatrix} x_3 \\ x_4 \\ h_3(x) - \frac{m_2 l_2^2 \beta x_3}{3\Delta} \\ h_4(x) + \frac{m_2 l_1 l_2 \beta c_2}{2\Delta} \end{bmatrix} + \begin{bmatrix} 0 \\ 0 \\ \frac{\mu m_2 l_2^2}{3\Delta} \\ \frac{-\mu m_2 l_1 l_2 c_2}{2\Delta} \end{bmatrix} u$$

where $s_k = sin(x_k)$, $c_k = cos(x_k)$ are used to simplify notation, and where:

$$h_3(x) = \frac{m_2^2 l_2^2 \left(-\frac{1}{2} g l_1 s_2 c_2 - \frac{1}{4} l_1 l_2 x_3^2 s_2 c_2^2 + b_2 l_1 x_4 c_2 / (m_2 l_2) + \frac{1}{3} l_1 l_2 x_4^2 s_2 - \frac{1}{3} l_2^2 x_3 x_4 s_2 c_2 \right)}{2\Delta}$$

$$h_4(x) = \frac{\frac{1}{2} m_2 g l_2 \left(m_2 l_1^2 + \frac{1}{4} m_2 l_2^2 s_2^2 + J_1 \right) s_2}{\Delta} - \frac{\left(m_2 l_1^2 + \frac{1}{4} m_2 l_2^2 s_2^2 + J_1 \right) b_2 x_4}{\Delta} + \frac{\frac{1}{4} m_2 l_2^2 [m_2 l_1^2 (x_3^2 - x_4^2) s_2 c_2 + \frac{1}{4} m_2 l_2^2 x_3^2 s_2^3 c_2 + J_1 x_3^2 s_2 c_2 + m_2 l_1 l_2 x_3 x_4 s_2 c_2^2]}{\Delta}$$

$$\Delta = m_2 l_2^2 \left(\frac{1}{3} m_2 l_1^2 + \frac{1}{12} m_2 l_2^2 s_2^2 + \frac{1}{3} J_1 - \frac{1}{4} m_2 l_1^2 c_2^2 \right).$$

9.2 Models and Parameters for Case Study 1

Luenberger observer with small gain :

$$L_{3-small} = \begin{bmatrix} 5.9207 & -7.4414 & -13.0209 & -9.9019 \\ -1.5356 & 21.6603 & -7.2493 & 108.1343 \end{bmatrix}^T .$$

High-gain Luenberger observer :

$$L_{3-large} = 10^3 \begin{bmatrix} 0.0716 & 0.0070 & 0.1432 & -0.5022 \\ 0.0203 & 0.2206 & 1.4312 & 4.4841 \end{bmatrix}^T .$$

Dynamic Lipschitz observer : (K_3, obtained for $\alpha = 44.45,\ \epsilon = \beta = 0.00048828$)

$$A_{L3} = 10^4 \begin{bmatrix} -0.3428 & 0 & 0 & 0 \\ 0 & -0.3428 & 0 & 0 \\ -6.2073 & 0 & -0.2048 & 0 \\ 0 & -6.2073 & 0 & -0.2048 \end{bmatrix},\ B_{L3} = 10^4 \begin{bmatrix} 0.138 & 0 \\ 0 & 0.138 \\ 6.2072 & 0 \\ 0 & 6.2072 \end{bmatrix},$$

$$C_{L3} = 10^3 \begin{bmatrix} 2.048 & 0 & 0.0005 & 0 \\ 0 & 2.048 & 0 & 0.0005 \\ 0.0005 & 0 & 2.0480 & \\ 0 & 0.0005 & 0 & 2.0485 \end{bmatrix},\ D_{L3} = \begin{bmatrix} 0 & 0 \\ 0 & 0 \\ 0 & 0 \\ 0 & 0 \end{bmatrix}.$$

Nonlinear "normal form" Controller :
By considering $y = x_2$, and using the nonlinear model of the ROTPEN in Appendix 9.1, the following coordinate transformation:

$$\begin{bmatrix} \xi_1 \\ \xi_2 \\ \eta_1 \\ \eta_2 \end{bmatrix} = \begin{bmatrix} x_2 \\ x_4 \\ x_1 \\ x_3 \left(\frac{l_1}{2} c_2\right) + x_4 \frac{l_2}{3} \end{bmatrix}$$

is used to put the system in the so-called *normal* or *tracking form* (Marino & Tomei, 1995), that is:

$$\begin{bmatrix} \dot{\xi}_1 \\ \dot{\xi}_2 \\ \dot{\eta}_1 \\ \dot{\eta}_2 \end{bmatrix} = \begin{bmatrix} \xi_2 \\ f_4(x) + g_4(x)u \\ x_3 \\ -\frac{l_1}{2} x_3 x_4 s_2 + \frac{l_1}{2} c_2 f_3(x) + \frac{l_2}{3} f_4(x) \end{bmatrix}$$

and using the control law:

$$u = \frac{1}{g_4(x)} \left[-9x_2 - 6x_4 - f_4(x)\right]$$

where $f_4(x)$ and $g_4(x)$ denote the 4^{th} elements of $f(x)$ and $g(x)$ in Appendix 9.1 respectively. The subsystem $(\xi_1,\ \xi_2)$ is then stabilized. It is important to note that the zero dynamics in this case, i.e the subsystem $(\eta_1,\ \eta_2)$ is unstable, and therefore the motor angle is not guaranteed to converge to the reference input.
Static Lipschitz observer : (obtained for $\alpha = 1,\ \varepsilon = 0.5$)

$$L_5 = \begin{bmatrix} 1.7108 & -2.1247 & 1.9837 & -5.4019 \\ 0.4338 & -0.2089 & 1.1030 & -2.8972 \end{bmatrix}^T .$$

9.3 Models and Parameters for Case Study 2

Lipschitz reduced-order model for observer design ($\bar{x} = [\theta_2\ \dot{\theta_1}\ \dot{\theta_2}]^T$) :

$$\dot{\bar{x}} = \begin{bmatrix} 0 & 0 & 1 \\ -25.14 & -17.22 & 0.2210 \\ 68.13 & 16.57 & -0.599 \end{bmatrix} \bar{x} + \begin{bmatrix} 0 \\ \phi_1(\bar{x}, u) \\ \phi_2(\bar{x}, u) \end{bmatrix}$$

$$\bar{y} = \begin{bmatrix} 1 & 0 & 0 \end{bmatrix} \bar{x}$$

Lipschitz dynamic observer for sensor bias : (K_6, obtained for $\lambda = 10^{-12}$, $\epsilon = 0.1$)

$$A_{L6} = \begin{bmatrix} -175.7353 & 3.8503 & 0.1710 & -30.6336 \\ 16.8182 & -171.9539 & 26.7652 & 32.1257 \\ 35.1361 & 16.5360 & -97.3465 & 114.1349 \\ -87.9041 & 25.7568 & 62.1442 & -87.8099 \end{bmatrix},\ B_{L6} = \begin{bmatrix} 5.0462 \\ -44.8932 \\ -75.4539 \\ 106.5497 \end{bmatrix},$$

$$C_{L6} = \begin{bmatrix} 167.6750 & -5.0531 & -8.5208 & 42.0138 \\ -7.1899 & 155.5373 & -42.6804 & -11.1441 \\ 5.3053 & -18.7128 & -120.8293 & 171.1055 \end{bmatrix},\ D_{L6} = \begin{bmatrix} 0 \\ 0 \\ 0 \end{bmatrix}.$$

Lipschitz dynamic observer for fault of 2 rad/sec : (K_7, obtained for $\lambda = 10^{-12}$, $\epsilon = 0.1$)

$$A_{L7} = \begin{bmatrix} -816.9997 & -12.5050 & -51.0842 & -64.0861 & 31.8003 \\ 23.8482 & -772.7024 & 149.1621 & 122.7602 & -75.3718 \\ -3.0714 & 139.9543 & -412.1421 & 361.2027 & -176.7926 \\ -193.3011 & 128.2831 & 346.2370 & -405.3024 & 201.2094 \\ 71.5547 & -47.7237 & -104.0209 & 129.8922 & -64.7247 \end{bmatrix},\ B_{L7} = \begin{bmatrix} 9.2096 \\ -73.6540 \\ -80.3861 \\ 177.6628 \\ -67.4227 \end{bmatrix},$$

$$C_{L7} = \begin{bmatrix} 809.4037 & 11.3091 & 28.1928 & 88.3295 & -43.7581 \\ -13.1309 & 758.2718 & -276.6110 & 4.7255 & 12.0717 \\ -15.9908 & -176.8554 & -509.7118 & 587.8999 & -294.7496 \end{bmatrix},\ D_{L7} = \begin{bmatrix} 0 \\ 0 \\ 0 \end{bmatrix}.$$

Lipschitz dynamic observer for low frequencies : (K_8, obtained for $\lambda = 10^{-12}$, $\epsilon = 0.1$)

$$A_{L8} = \begin{bmatrix} -217.7814 & 1.8898 & -4.8573 & -38.2385 \\ -1.5288 & -185.0261 & 38.1186 & 36.8585 \\ 108.5437 & 28.4810 & -87.0920 & 135.1710 \\ -618.9648 & 28.9348 & 82.1016 & -164.6086 \end{bmatrix},\ B_{L8} = \begin{bmatrix} -30.2950 \\ 26.3896 \\ 147.7784 \\ -637.5223 \end{bmatrix},$$

$$C_{L8} = \begin{bmatrix} -184.6168 & 3.4213 & 1.8716 & -51.2266 \\ 6.5728 & -171.5615 & 49.1851 & 16.3542 \\ -4.3022 & 15.0586 & 114.2413 & -224.5769 \end{bmatrix},\ D_{L8} = \begin{bmatrix} 0 \\ 0 \\ 0 \end{bmatrix}.$$

10. References

Aboky, C., Sallet, G. & Vivalda, J. (2002). Observers for Lipschitz nonlinear systems, *Int. J. of Contr.*, vol. 75, No. 3, pp. 204-212.

Adjallah, K., Maquin, D. & Ragot, J. (1994). Nonlinear observer based fault detection, *IEEE Trans. on Automat. Contr.*, pp. 1115-1120.

Chen, R., Mingori, D. & Speyer, J. (2003). Optimal stochastic fault detection filter, *Automatica*, vol. 39, No. 3, pp. 377-390.

Chen, J. & Patton, R. (1999). *Robust model-based fault diagnosis for dynamic systems*, Kluwer Academic Publishers.

Doyle, J., Glover, K., Khargonekar P. & Francis, B. (1989). State spce solutions to standard H_2 and H_∞ control problems, *IEEE Trans. Automat. Contr.*, Vol. 34, No. 8, pp. 831-847.

Frank, P. (1990). Fault diagnosis in dynamic systems using analytical and knowledge-based redundancy - A survey and some new results, *Automatica*, vol. 26, No. 3, pp. 459-474.

Gahinet, P. & Apkarian, P. (1994). A linear matrix inequality approach to H_∞ control, *Int. J. of Robust and Nonlinear Contr.*, vol. 4, pp. 421-448.

Garcia, E. & Frank, P. (1997). Deterministic nonlinear observer based approaches to fault diagnosis: A survey, *Contr. Eng. Practice*, vol. 5, No. 5, pp. 663-670.

Hammouri, H., Kinnaert, M. & El Yaagoubi, E. (1999). Observer-based approach to fault detection and isolation for nonlinear systems, *IEEE Trans. on Automat. Contr.*, vol. 44, No. 10.

Hill, D. & Moylan, P. (1977). Stability Results for Nonlinear Feedback Systems, *Automatica*, Vol. 13, pp. 377-382.

Iwasaki, T. & Skelton, R. (1994). All controllers for the general H_∞ control problem: LMI existence conditions and state space formulas, *Automatica*, Vol. 30, No. 8, pp. 1307-1317.

Kabore, P. & Wang, H. (2001). Design of fault diagnosis filters and fault-tolerant control for a class of nonlinear systems, *IEEE Trans. on Automat. Contr.*, vol. 46, No. 11.

Lynch, A. (2004). *Control Systems II (Lab Manual)*, University of Alberta.

Marino, R. & Tomei, P. (1995). *Nonlinear Control Design - Geometric, Adaptive and Robust*, Prentice Hall Europe, 1995.

Marquez, H. (2003). *Nonlinear Control Systems: Analysis and Design*, Wiley, NY.

Pertew, A. (2006). Nonlinear observer-based fault detection and diagnosis, *Ph.D Thesis*, Department of Electrical and Computer Engineering, University of Alberta.

Pertew, A., Marquez, H. & Zhao, Q. (2005). H_∞ synthesis of unknown input observers for nonlinear Lipschitz systems, *International J. Contr.*, vol. 78, No. 15, pp. 1155-1165.

Pertew, A., Marquez, H. & Zhao, Q. (2006). H_∞ observer design for Lipschitz nonlinear systems, *IEEE Trans. on Automat. Contr.*, vol. 51, No. 7, pp. 1211-1216.

Pertew, A., Marquez, H. & Zhao, Q. (2007). LMI-based sensor fault diagnosis for nonlinear Lipschitz systems, *IEEE Trans. on Automat. Contr.*, vol. 43, pp. 1464-1469.

Raghavan, S. & Hedrick, J. (1994). Observer design for a class of nonlinear systems, *Int. J. of Contr.*, vol. 59, No. 2, pp. 5515-528.

Rajamani, R. (1998). Observers for Lipschitz nonlinear systems, *IEEE Trans. on Automat. Contr.*, vol. 43, No. 3, pp. 397-401.

Rajamani, R. & Cho, Y. (1998). Existence and design of observers for nonlinear systems: relation to distance of unobservability, *Int. J. Contr.*, Vol. 69, pp. 717-731.

Scherer, C. (1992). H_∞ optimization without assumptions on finite or infinite zeros, *Int. J. Contr. and Optim.*, Vol. 30, No. 1, pp. 143-166.

Sciavicco, L. & Sicliano, B. (1989). Modeling and Control of Robot Manipulators, McGraw Hill.

Stoorvogel, A. (1996). The H_∞ control problem with zeros on the boundary of the stability domain, *Int. J. Contr.*, Vol. 63, pp. 1029-1053.

Vemuri, A. (2001). Sensor bias fault diagnosis in a class of nonlinear systems, *IEEE Trans. on Automat. Contr.*, vol. 46, No. 6.

Wang, H., Huang, Z. & Daley, S. (1997). On the Use of Adaptive Updating Rules for Actuator and Sensor Fault Diagnosis, *Automatica*, Vol. 33, No. 2, pp. 217-225.

Willsky, A. (1976). A survey of design methods for failure detection in dynamic systems, *Automatica*, vol. 12, pp. 601-611.

Yu, D. & Shields, D. (1996). A bilinear fault detection observer, *Automatica*, vol. 32, No. 11, pp. 1597-1602.

Zhong, M., Ding, S., Lam, J. & Wang, H. (2003). An LMI approach to design robust fault detection filter for uncertain LTI systems, *Automatica*, vol. 39, No. 3, pp. 543-550.

Zhou, K. & Doyle, J. (1998). *Essentials of robust control*, Prentice-Hall, NY.

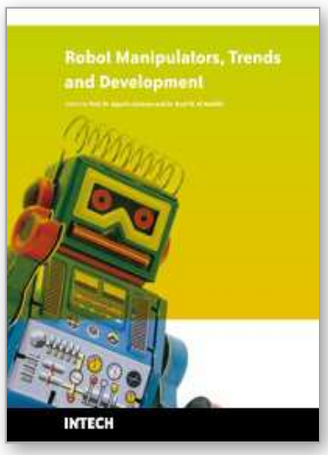

Robot Manipulators Trends and Development

Edited by Agustin Jimenez and Basil M Al Hadithi

ISBN 978-953-307-073-5
Hard cover, 666 pages
Publisher InTech
Published online 01, March, 2010
Published in print edition March, 2010

This book presents the most recent research advances in robot manipulators. It offers a complete survey to the kinematic and dynamic modelling, simulation, computer vision, software engineering, optimization and design of control algorithms applied for robotic systems. It is devoted for a large scale of applications, such as manufacturing, manipulation, medicine and automation. Several control methods are included such as optimal, adaptive, robust, force, fuzzy and neural network control strategies. The trajectory planning is discussed in details for point-to-point and path motions control. The results in obtained in this book are expected to be of great interest for researchers, engineers, scientists and students, in engineering studies and industrial sectors related to robot modelling, design, control, and application. The book also details theoretical, mathematical and practical requirements for mathematicians and control engineers. It surveys recent techniques in modelling, computer simulation and implementation of advanced and intelligent controllers.

How to reference

In order to correctly reference this scholarly work, feel free to copy and paste the following:

Amr Pertew Ph.D P.Eng., Horacio Marquez Ph.D P.Eng and Qing Zhao Ph.D P.Eng (2010). Measurement Analysis and Diagnosis for Robot Manipulators Using Advanced Nonlinear Control Techniques, Robot Manipulators Trends and Development, Agustin Jimenez and Basil M Al Hadithi (Ed.), ISBN: 978-953-307-073-5, InTech, Available from: http://www.intechopen.com/books/robot-manipulators-trends-and-development/measurement-analysis-and-diagnosis-for-robot-manipulators-using-advanced-nonlinear-control-technique

INTECH
open science | open minds

InTech Europe
University Campus STeP Ri
Slavka Krautzeka 83/A
51000 Rijeka, Croatia
Phone: +385 (51) 770 447
Fax: +385 (51) 686 166
www.intechopen.com

InTech China
Unit 405, Office Block, Hotel Equatorial Shanghai
No.65, Yan An Road (West), Shanghai, 200040, China
中国上海市延安西路65号上海国际贵都大饭店办公楼405单元
Phone: +86-21-62489820
Fax: +86-21-62489821

IntechOpen